Electronic Supporting Information (ESI)

Tunable photoluminescence in van der Waals heterojunction built from MoS_2 monolayer and PTCDA organic semiconductor

Mohammad Rezwan Habib,[a] Hongfei Li,[b] Yuhan Kong,[b] Tao Liang,[b] Sk. Md. Obaidulla,[a] Shuang Xie,[c] Shengping Wang,[c] Xiangyang Ma,[c] Huanxing Su*[d] and Mingsheng Xu*[a]

[a] State Key Laboratory of Silicon Materials, College of Information Science & Electronic Engineering, Zhejiang University, Hangzhou 310027, P. R. China.

[b] Department of Polymer Science and Engineering, Zhejiang University, Hangzhou 310027, P. R. China.

[c] State Key Laboratory of Silicon Materials, School of Materials Science and Engineering, Zhejiang University, Hangzhou 310027, P. R. China

[d] State Key Laboratory of Quality Research in Chinese Medicine and Institute of Chinese Medical Sciences, University of Macau, Macau SAR, P. R. China.

* msxu@zju.edu.cn, huanxingsu@umac.mo

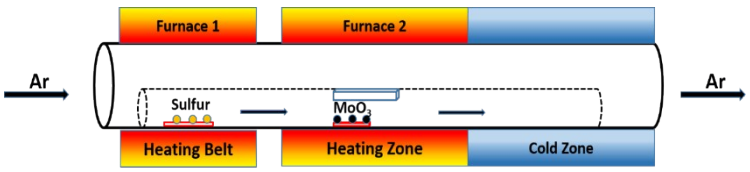

Figure S1. Schematic illustration of the CVD system for MoS_2 synthesis.

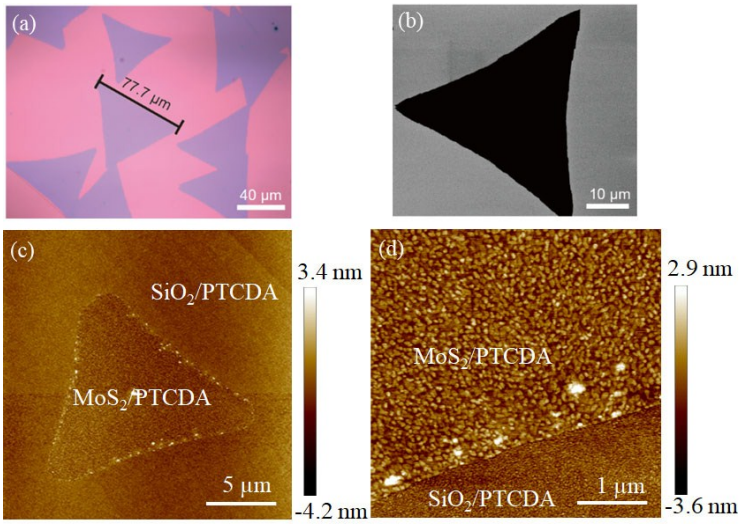

Figure S2. Structural characterization of monolayer MoS_2 synthesized by CVD. (a) An optical microscope image of MoS_2 sheets on Si/SiO_2. (b) SEM image of MoS_2 on Si/SiO_2. (c) and (d) AFM topographic images of PTCDA on MoS_2 sheets as well as on bare SiO_2.

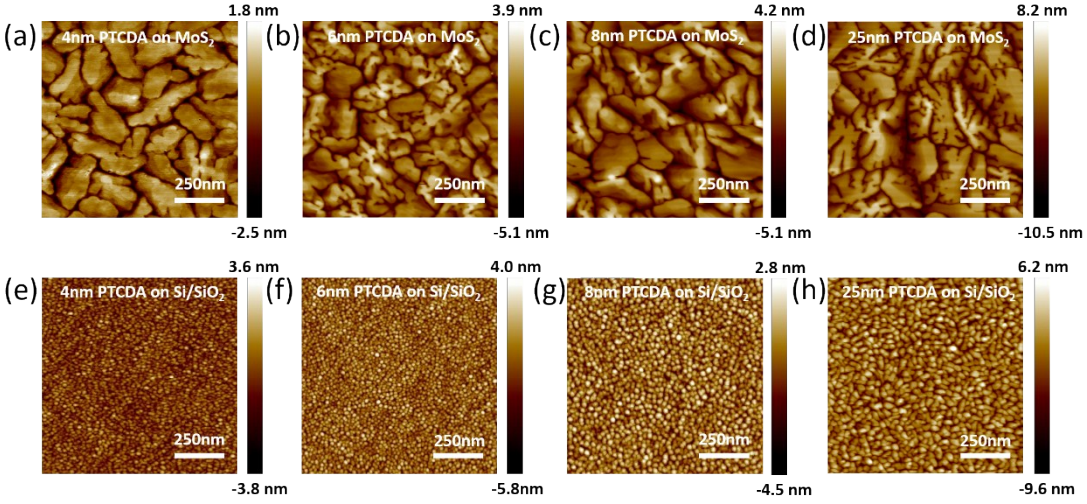

Figure S3. Morphological comparison of PTCDA films with different thickness (4 nm, 6 nm, 8 nm, and 25 nm) on MoS_2 (a-d) and Si/SiO_2 surfaces (e-h).

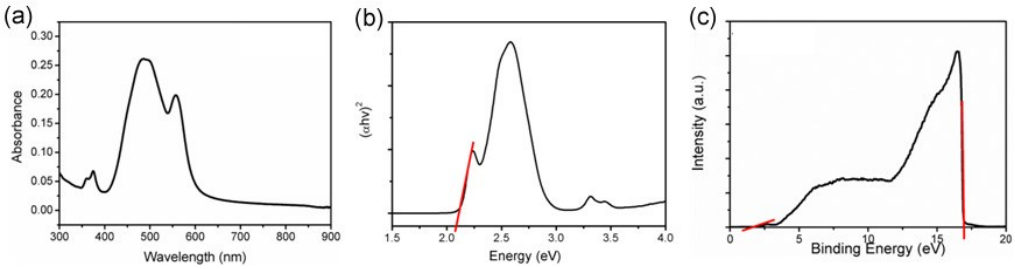

Figure S4. (a) UV-vis absorbance spectrum of PTCDA film. (b) Plot of $(\alpha h\nu)^2$ as a function of energy based on $\alpha h\nu = C(h\nu - E_g)^{1/2}$ according to (a). (c) Ultraviolet photoelectron spectroscopy (UPS) spectrum of the PTCDA film.

To estimate the optical bandgap of PTCDA film, we reploted the UV-vis absorption spectrum of the PTCDA film by using the Tauc equation[S1] of $\alpha h\nu = C(h\nu - E_g)^{1/2}$, where where α, h, ν, C, and E_g are the absorption coefficient, Planck's constant, the incident light frequency, proportionality constant, and the band-gap energy, respectively. Thus, band-gap energy (~2.1 eV) of the PTCDA film can be thus estimated from a plot of $(\alpha h\nu)^2$ versus the photon energy ($h\nu$), where in the graph the intercept is the band gap as shown by the red straight line.

Based on the UPS result in Figure S3c, the HOMO level of the PTCDA film is determined[S2,S3] to be about 6.73 eV. That is, the two red lines are the tangents to the curve, which show the position of the Fermi and the cut-off edge. From the UPS image, we can get the E_{Fermi} is around at 2.43 eV and the $E_{cut\text{-}off}$ is around at 16.92 eV. So we can calculate the E_{HOMO} by using the formula $E_{HOMO} = 21.22 - (16.92 - 2.43) = 6.73$ eV. Combining UV-Vis measurements to measure or calculate band gap of PTCDA film and UPS measurements of the HOMO, the LUMO of PTCDA film can be determined at about 4.62 eV and the band structure diagram can be easily drawn.

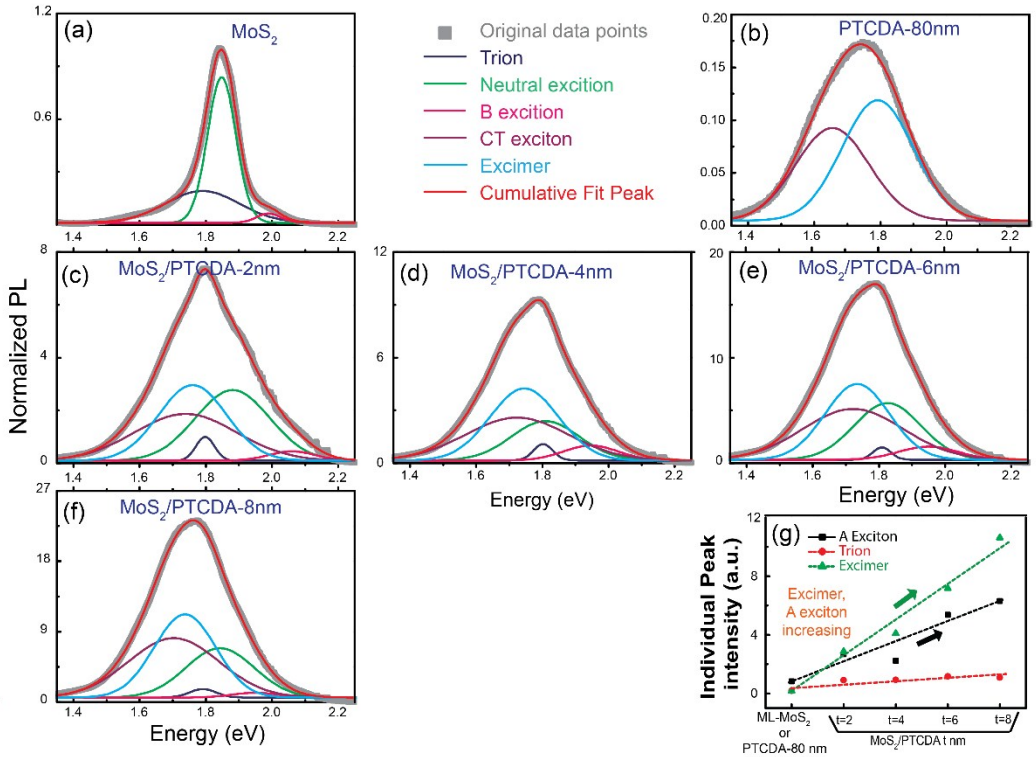

Figure S5. PL peak deconvolution. Normalized PL spectra of (a) monolayer MoS_2 and (b) 80 nm PTCDA film on SiO_2/Si substrate and (c-f) PL spectra of 2 nm, 4 nm, 6 nm, and 8 nm PTCDA film on MoS_2. The grey thick curves represent the corresponding experimental results and the red lines are the fitted. Normalization of all PL spectra has been done with respect to the PL spectra of monolayer MoS_2 to show the contribution of individual PL peaks to total intensity compare to ML MoS_2. The PL peak could be deconvoluted into five components due to A exciton or neutral exciton (green), B exciton (pink), A^- trion (blue), CT exciton (purple) and excimer (cyan). A, B and A^- are PL emission channels of MoS_2 and CT, excimer emission channels for PTCDA films. (g) Peak intensity of A exciton and excimer are increased in MoS_2/PTCDA heterostructure compare to ML-MoS_2.

Kobitski *et al*. [S4] reported that at room temperatures, PL channels of PTCDA such as Frenkel and S band are quenched due to activated nonradiative decay mechanisms, and the CT exciton and excimer PL become the important radiative recombination channels because the influence of nonradiative processes on the recombination rate is much weaker than for the other PL bands.

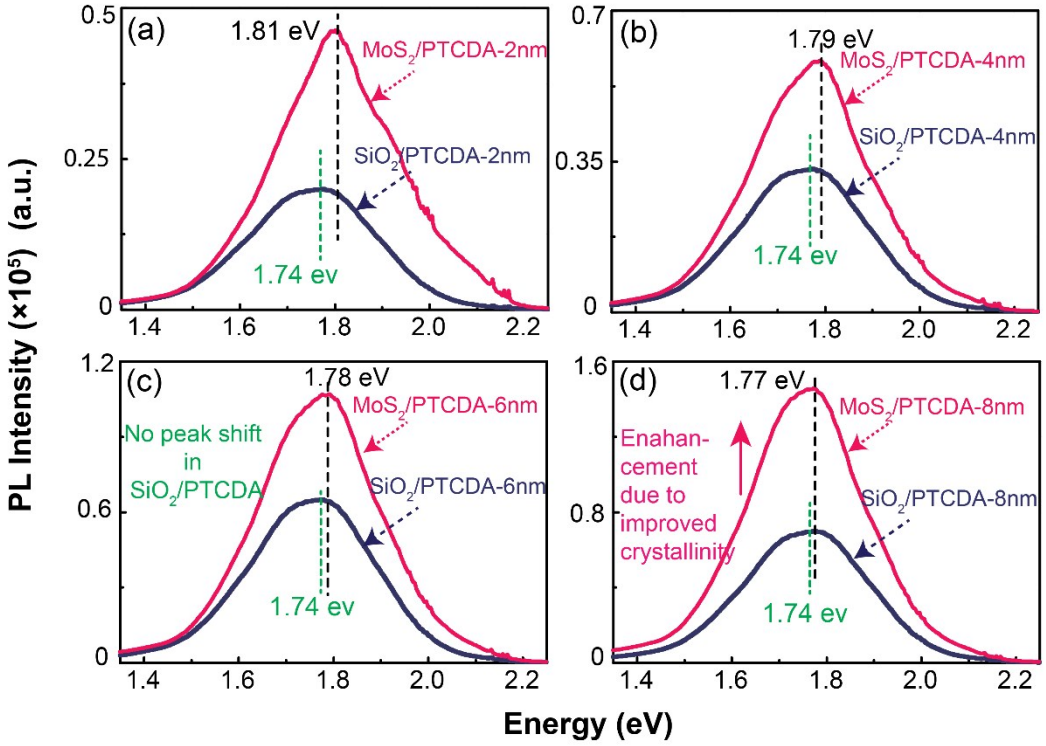

Figure S6: Comparison of PL of PTCDA film of different thickness 2nm (a), 4 nm (b), 6nm (c), and 8nm (d) on both MoS_2 and SiO_2.

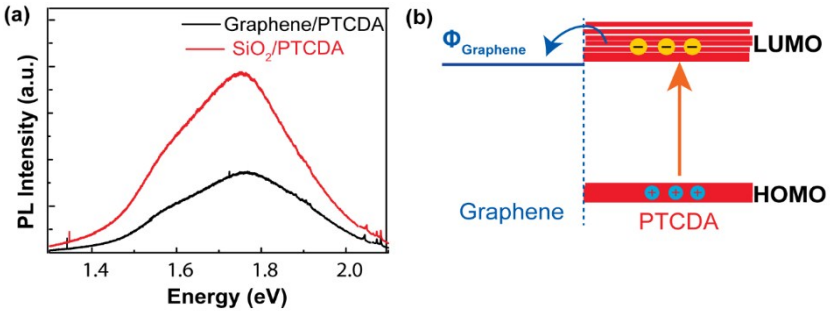

Figure S7. (a) PL quenching of PTCDA on graphene, (b) Energy level diagram of graphene and PTCDA.

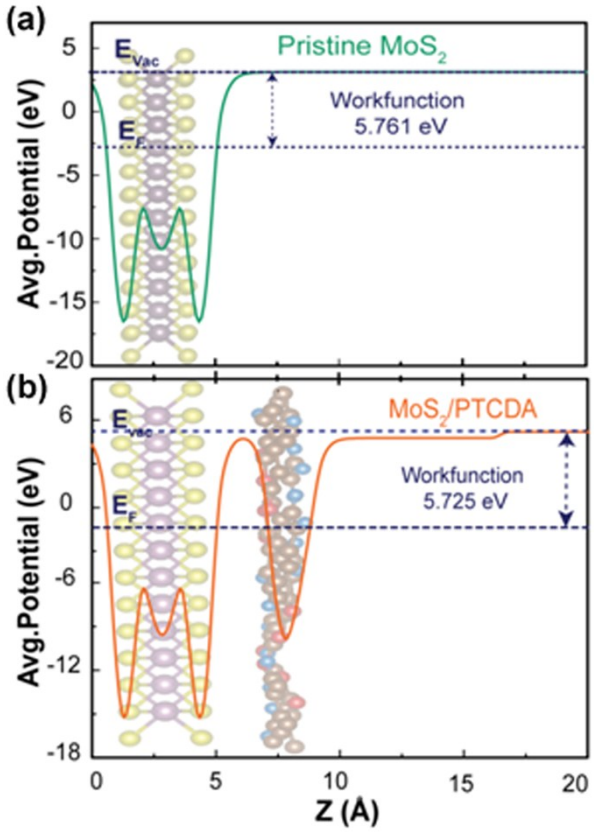

Figure S8. Plane averaged electrostatic potential calculation to show the possibility of interfacial charge transfer. (a) Plane averaged electrostatic potential of MoS_2. (b) Plane averaged electrostatic potential of MoS_2/PTCDA heterostructure. E_{vac} and E_F represent the vacuum level and Fermi level, respectively. Workfunctions, difference between vacuum level and Fermi level, of the pristine monolayer MoS_2 and MoS_2/PTCDA heterostructure are 5.761 eV and 5.725 eV, respectively. Side view of pristine MoS_2 and MoS_2/PTCDA heterostructure are shown in the background of (a) and (b), respectively.

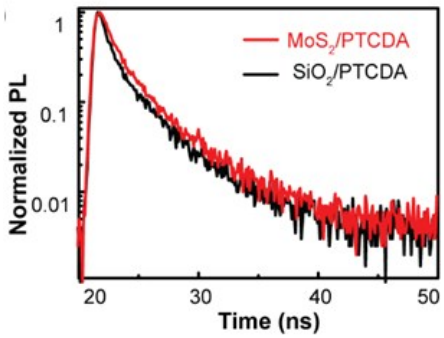

Figure S9. Time-resolved PL spectra of the PTCDA film on Si/SiO_2 substrate and MoS_2.

The decay transients can be fitted using a biexponential decay function expressed as follows [S5,S6]:

$$I(t) = A_1 exp(-t/\tau_1) + A_2 exp(-t/\tau_2)$$

where A_1 and A_2 are the amplitudes (or weighting factors), and τ_1 and τ_2 are the corresponding lifetimes.

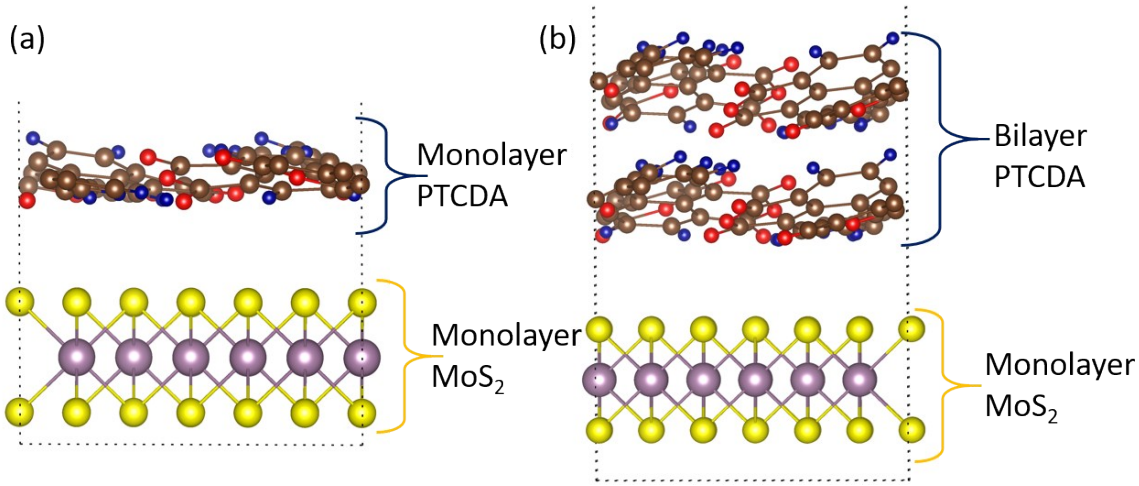

Fig. S10: Optimized structure of monolayer (a) and bilayer PTCDA (b) on monolayer MoS_2.

Explanation of Raman peak shift related to interaction between the MoS_2/PTCDA

The shift observed in MoS_2/PTCDA heterostructure can be attributed to the interlayer interaction between MoS_2 and PTCDA layer. The shifting of A_{1g} peak (out of plane vibration) has similar explanation with the layer-dependent Raman shift in MoS_2.[S7] The position of a phonon with momentum **q** and pos **(q)** in condensed material can be written as:

$$\left| (1/\sqrt{M_m M_n}) \sum C_{m\alpha, n\beta}(\mathbf{q}) - pos^2(\mathbf{q}) \right| = 0 \qquad (1)$$

where M_m and M_n are the mass of m^{th} and n^{th} atoms, respectively, involved in the vibration and $C_{m\alpha, n\beta}(\mathbf{q})$ corresponds to real space atomic force constant matrix. α and β represent the direction of the vibration of atoms m and n, respectively. The interlayer interaction term of MoS_2 (for bilayer, trilayer and so on) is represented by matix element $C_{SzSz'}$. Zhou *et al*.[S2] modelled this interaction term by a spring which connect two sulfur atoms. So for bare monolayer MoS_2 the phonon position of A_{1g} peak is equal to $[1/Ms(C_{Sz,Sz})]^{1/2}$. The introduction of PTCDA layer on MoS_2 introduces an additional term ($C_{Sz,Cz'}$) due to the interaction between the MoS_2 and PTCDA layer (confirmed by projected density of state). This additional term increases the phonon position of A_{1g} up to $[1/Ms(C_{Sz,Sz}+C_{Sz,Cz'})]^{1/2}$ and shifted to higher wavenumber compare to monolayer MoS_2. The blue shifting for the 6 nm and 8 nm PTCDA film-based MoS_2/PTCDA heterostructures are less compared to the 2 nm and 4 nm (similar trend for thicker MoS_2 film i.e. for 5L and 6L MoS_2 A_{1g} peak shift is less compared to 2L and 3L MoS_2) can be explained by the competition between the vdW interaction of MoS_2 and PTCDA layer and intermolecular interaction of PTCDA layers which confirmed by layer dependent binding energy of PTCDA on MoS_2 (see in the main text). For higher PTCDA thickness the vdW interaction between MoS_2 and PTCDA layer is suppressed by the intermolecular interaction of PTCDA. This also explain the observation of the enhancement of the PL intensity with negligible peak shift of the MoS_2/PTCDA when the PTCDA film was thick enough.

[S1] J. Tauc, in: Amorphous and Liquid Semiconductors, Plenum, 1974, p. 159.

[S2] Seki, et al. Trans. on Electron Dev. 1997, 44, 1295.

[S3] Handbook of x-ray and ultraviolet photoelectron spectroscopy, edited by D. Briggs, Heyden&Son Ltd, 1977.

[S4] A. Y. Kobitski, R. Scholz, D. R. T. Zahn, H. P. Wagner, *Phys. Rev. B* 2003, 68, 155201.

[S5] X. Liu, Q. Zhang, G. Xing, Q. Xiong, and T. C. Sum, *J. Phys. Chem. C* 2013, 117, 10716.

[S6] C.Y. Luan, S. Xie, C. Y. Ma, S. P. Wang, Y. H. Kong, M. S. Xu, *Appl. Phys. Lett.* 2017, 111, 073105.

[S7] K. G. Zhou, F. Withers, Y. Cao, S. Hu, G. L. Yu, C. Casiraghi, *ACS Nano* 2014, 8, 9914.